AIMS Mathematics, 8(5): 11180–11201.
DOI: 10.3934/math.2023566
Received: 24 December 2022
Revised: 16 February 2023
Accepted: 22 February 2023
Published: 09 March 2023

http://www.aimspress.com/journal/Math

Research article

Fractionalizing, coupling and methods for the coupled system of two-dimensional heat diffusion models

Rahmatullah Ibrahim Nuruddeen[1], **J. F. Gómez-Aguilar** [2,*] **and José R. Razo-Hernández**[3]

[1] Department of Mathematics, Federal University Dutse, Jigawa State, Nigeria
[2] CONACyT-Tecnológico Nacional de México/CENIDET, Interior Internado Palmira S/N, Col. Palmira, C.P. 62490 Cuernavaca, Morelos, México
[3] Departamento de Ingeniería Electromecánica, Tecnológico Nacional de México, Instituto Tecnológico Superior de Irapuato (ITESI), Carr. Irapuato-Silao km 12.5, Colonia El Copal, C.P. 36821, Irapuato, Guanajuato, México

* **Correspondence:** Email: jose.ga@cenidet.tecnm.mx; Tel: +527773627770.

Abstract: The present manuscript gives an overview of how two-dimensional heat diffusion models underwent a fractional transformation, system coupling as well as solution treatment. The governing diffusion models, which are endowed with Caputo's fractional-order derivatives in time t, are suitably coupled using the (1) convection phenomenon, (2) interfacial coupling by considering the mechanism of a double-layered bar, and the (3) nonlinear coupling due to temperature-dependent thermal diffusivities. Semi-analytical and analytical methods are considered for the solution treatment. Moreover, we seek a computational environment to graphically illustrate the systems' response to different fractional orders in each case through the determined diffusional fields. Besides, we supply certain concluding notes at the end.

Keywords: fractionalization; couplings; integral transforms; Laplace decomposition method; heat diffusion models
Mathematics Subject Classification: 26A33, 34A08, 34K37, 35R11

1. Introduction

Heat diffusion procedures have been comprehensively examined in both the fast and current literature owing to their enormous uses. The area is still hot and remains fresh on the minds of many researchers owing to the present technological progress. A very good account of the heat conduction, as well as diffusion procedures in solid media like bars, cylinders, composites, and shells,

can be seen in the work of Carslaw and Jaeger [1]; see also [2–4] and the cited papers therein. Nevertheless, with the current energetic return of the fractional derivative theory [5–10], after being stuck in the past decades, a lot of scientists have shifted their inquisitiveness to the study of heat diffusion/conduction processes within the framework of fractional calculus. Thus, various analytical and approximation methods have been devised and utilized to scrutinize the governing models. For instance, Yan et al. [11] have proposed a series solution method and further applied it to a class of diffusion equations featuring fractional-order derivatives. We also recall the work by Al-Khaled and Momani [12] on the determination of approximate solutions of wave-diffusion equations endowed with fractional orders. More so, we summarily mention some relevant examinations with regard to the relevance of fractional-order derivatives in the theory, as well as in the application of heating processes, including, the nonlinear heat transfer process, comparative examination of the conformable and Caputo fractional-orders with regard to the nonlocal heat equation, and the correlation between the nonlinearity and fractional-order derivative in diffusion equations to mentioned a few; all by the modification of Adomian decomposition methods [13–18]. We also make mention of Lie's method of symmetry for the two-dimensional diffusion model [19], the integral transformation, and other methods [20–30] to mention a few.

Moreover, with the re-birth of the fractional calculus theory, together with its contemporary applications in modern science and technology, the present study aims to propose three different couplings for the heat diffusion models; of course, after being fractionalized. To do this, we first seek two separate diffusion equations that were initially examined with nonlocal boundary conditions by Bokhari et al. [15] Indeed, the models with their respective exact analytical solutions take the following expressions:

$$\text{Model I:} \quad \begin{cases} \frac{\partial w_1}{\partial t} = \frac{\partial^2 w_1}{\partial x^2} + \frac{\partial^2 w_1}{\partial y^2}, \\ \\ w_1(x, y, t) = e^{-2t} \sin(x) \sin(y), \end{cases} \tag{1.1}$$

$$\text{Model II:} \quad \begin{cases} \frac{\partial w_2}{\partial t} = \frac{\partial^2 w_2}{\partial x^2} + \frac{\partial^2 w_2}{\partial y^2}, \\ \\ w_2(x, y, t) = e^{-2t} \sin(x + y), \end{cases} \tag{1.2}$$

where $w_1 = w_1(x, y, t)$ and $w_2 = w_2(x, y, t)$ are the respective dimensionless diffusional fields; and all the physical as well as the material properties are considered to be unity. Such diffusion models are found to model various physical phenomena in thermoelasticity [1]; in addition to their relevance in nonlocal scenarios [15].

Additionally, when the models given in Eqs (1.1) and (1.2) are fractionalized in time t, using the Caputo's fractional derivative definition with $0 < \alpha \leq 1$, the models thus become [18]:

$$\text{Fractionalized model I:} \quad \begin{cases} \frac{\partial^\alpha w_1}{\partial t^\alpha} = \frac{\partial^2 w_1}{\partial x^2} + \frac{\partial^2 w_1}{\partial y^2}, \ \ 0 < \alpha \leq 1, \\ \\ w_1(x, y, t) = E_\alpha(-2t) \sin(x) \sin(y), \end{cases} \tag{1.3}$$

$$\text{Fractionalized model II:} \quad \begin{cases} \frac{\partial^\alpha w_2}{\partial t^\alpha} = \frac{\partial^2 w_2}{\partial x^2} + \frac{\partial^2 w_2}{\partial y^2}, \ \ 0 < \alpha \leq 1, \\ \\ w_2(x, y, t) = E_\alpha(-2t) \sin(x + y). \end{cases} \tag{1.4}$$

where $E_\alpha(.)$ in Eqs $(1.3)_2$ and $(1.4)_2$ is the one-parameter Mittag-Leffler function that is explicitly defined by [16,18]

$$E_\alpha(t) = \sum_{n=0}^{\infty} \frac{t^n}{\Gamma(\alpha n + 1)}, \quad \alpha > 0, \quad t \in \mathbb{C}, \tag{1.5}$$

with $\Gamma(.)$ denoting the Gamma function, and further takes the following definition:

$$\Gamma(z) = (z-1)! = \int_0^\infty t^{z-1} e^{-t} dt. \tag{1.6}$$

However, the current manuscript is arranged as follows: some basics about the fractional-order calculus and the aiming methodologies are given in Section 2; while Section 3 gives the statement of the problem. The application of the delineated methodology is given in Section 4, and lastly, Section 5 presents the concluding points.

2. Preludes and methods

The current section gives some important preludes on the fractional calculus that would be utilized in the study. Also, the section recalls the definitions of the classical Laplace and Fourier transforms alongside their inverses. Further, the Laplace Adomian decomposition methodology is also reviewed.

2.1. Fractional derivative

The current study makes consideration of Caputo's fractional derivative [16,20]. More so, Caputo's fractional derivative is the most widely used fractional derivative after Riemann-Liouville's derivative; the two (Caputo and Riemann-Liouville) are also the pioneers.

Therefore, the fractional-order derivative definition based on Caputo's definition of a function $w(t)$ is given by [16,18,20],

$$D_t^\alpha w(t) = \frac{1}{\Gamma(n-\alpha)} \int_0^t \frac{w^{(n)}(s)}{(t-s)^{\alpha+1-n}} ds, \qquad n-1 < \alpha \leqslant n. \tag{2.1}$$

Consequently, we deduce the following properties from the above definition:

(1) $D_t^\alpha(\text{constant}) = 0$,
(2) $D_t^\alpha t^\beta = \frac{\Gamma(\beta+1)}{\Gamma(\beta-\alpha+1)} t^{\beta-\alpha}$,
(3) $D_t^\alpha\left(cw(t)\right) = cD_t^\alpha w(t), c$ constant,
(4) $D_t^\alpha\left(c_1 w_1(t) + c_2 w_2(t)\right) = c_1 D_t^\alpha\left(w_1(t)\right) + c_2 D_t^\alpha\left(w_2(t)\right), c_1, c_2$ constants,
(5) $D_t^\alpha(w(t)) = I^{1-\alpha}\left(\frac{d}{dt} w(t)\right)$, where

$$I^\alpha(w(t)) = \frac{1}{\Gamma(\alpha)} \int_0^t \frac{w(s)}{(t-s)^{1-\alpha}} ds,$$

(6) $D_t^\alpha(w(t)) = \bar{D}_t^\alpha(w(t)) - w(0)\frac{t^{-\alpha}}{\Gamma(1-\alpha)}$,

where $\bar{D}_t^\alpha$ in (6) is the Riemann-Liouville's operator; while α in (5) and (6) belong to $0 < \alpha \leq 1$.

2.2. Integral transforms

As we are going to utilize both the Fourier and Laplace transforms in the present study, the formal definitions of these transforms are outlined in the present subsection.

2.2.1. Fourier transform

The Fourier transform of a given function $w(x, y, t)$ in x-variable and its analogous inverse Fourier transform are sequentially defined as [22],

$$\begin{aligned} \mathfrak{F}\{w(x,y,t)\} &= \bar{w}(q,y,t) = \frac{1}{\sqrt{2\pi}}\int_{-\infty}^{\infty} e^{-iqx} w(x,y,t)dx, \\ \mathfrak{F}^{-1}\{\bar{w}(q,y,t)\} &= w(x,y,t) = \frac{1}{\sqrt{2\pi}}\int_{-\infty}^{\infty} e^{iqx} \bar{w}(q,y,t)dq, \end{aligned} \tag{2.2}$$

where q is the Fourier transform parameter.

2.2.2. Laplace transform

The Laplace transform of a given function $w(x, y, t)$ in t-variable and its analogous inverse Laplace transform are sequentially defined as [21,22],

$$\begin{aligned} \mathfrak{L}\{w(x,y,t)\} &= w^*(x,y,s) = \int_0^{\infty} e^{-st} w(x,y,t)dt, \quad \mathrm{Re}(s) > 0, \\ \mathfrak{L}^{-1}\{w^*(x,y,s)\} &= w(x,y,t) = \frac{1}{2\pi i}\int_{c-i\infty}^{c+i\infty} e^{st} w^*(x,y,s)ds, \quad c > 0, \end{aligned} \tag{2.3}$$

where s is the Laplace transform parameter. Moreover, in both transforms given in Eqs (2.2) and (2.3), the operators $\mathfrak{L}$, $\mathfrak{L}^{-1}$, $\mathfrak{F}$ and $\mathfrak{F}^{-1}$ are all linear operators.

Also, from Eq (2.3), we consequently deduce the Laplace transform in favour of Caputo's fractional operator of the function $w(x, y, t)$ with respect to t as follows [18]

$$\mathfrak{L}\{D_t^{\alpha} w(x,y,t)\} = s^{\alpha} w^*(x,y,s) - \sum_{k=0}^{n-1} s^{\alpha-k-1} w^{(k)}(x,y,0), \quad n-1 < \alpha \leqslant n. \tag{2.4}$$

In the same vein, we mention here that the inversion process of the Laplace transform would be carried out numerically whenever the analytical procedure fails; in fact, the methodology by Abate and Valkó [31] would be adopted. Such numerical inversion process is widely used in the literature for inverting the expected solution back to its original domain; see Nuruddeen [32], Ahmed et al. [33] and others [34,35] to mention a few. Moreover, other inversion schemes also exist like the Stehfest algorithm [36,37] among others.

2.3. Laplace Adomian decomposition approach

We present the Laplace Adomian decomposition approach based on the original Adomian method [23–30] to solve the formulated fractional models. In light of this, we make consideration

of the following two-dimensional nonhomogeneous nonlinear time-fractional differential equation to demonstrate the method,

$$D_t^{\alpha} w(x,y,t) = Lw(x,y,t) + Nw(x,y,t) + h(x,y,t), \qquad 0 < \alpha \leq 1, \tag{2.5}$$

coupled with the following initial data:

$$w(x,y,0) = g(x,y), \tag{2.6}$$

where in the above equations L is the linear differential operator, N is the nonlinear operator; while $h(x,y,t)$ is the nonhomogeneous term, and $g(x,y)$ is the prescribed moving initial data.

Thus, with the attendance of Caputo's fractional operator in Eq (2.5), this necessitates the application of the Laplace integral transform (in t-variable) coupled with the relation given in Eq (2.4) and the initial data in Eq (2.6) to get

$$w^*(x,y,s) = s^{-1}g(x,y) + s^{-\alpha}\mathfrak{L}\left(Lw(x,y,t) + Nw(x,y,t)\right) + s^{-\alpha}\mathfrak{L}(h(x,y,t)). \tag{2.7}$$

What's more, upon applying the inverse Laplace transform to both sides of the later equation (in s), it then yields

$$w(x,y,t) = g(x,y) + \mathfrak{L}^{-1}\left(s^{-\alpha}\left(\mathfrak{L}(h(x,y,t))\right)\right) + \mathfrak{L}^{-1}\left(s^{-\alpha}\mathfrak{L}\left(Lw(x,t) + Nw(x,t)\right)\right). \tag{2.8}$$

Then, on using the standard Adomian approach [28], the solution $w(x,y,t)$ and the nonlinear term $Nw(x,y,t)$ are then decomposed via the summation of infinite series of components as follows

$$w(x,y,t) = \sum_{n=0}^{\infty} w_n(x,y,t), \qquad Nw(x,y,t) = \sum_{n=0}^{\infty} A_n, \tag{2.9}$$

where A_n's are the polynomials by Adomian, which will then be recursively determined via the application of the Adomian's relation [28]. Further, upon substituting Eq (2.9) into Eq (2.8), we get the following recursive scheme for the problem:

$$\begin{cases} w_0(x,y,t) = g(x,y) + \mathfrak{L}^{-1}\left(s^{-\alpha}\left(\mathfrak{L}(h(x,y,t))\right)\right), & k = 0, \\ w_{k+1}(x,y,t) = \mathfrak{L}^{-1}\left(s^{-\alpha}\mathfrak{L}\left(L\left(w_k(x,y,t)\right) + A_k\right)\right), & k \geq 0, \end{cases} \tag{2.10}$$

where the first component $w_0(x,y,t)$ is associated with the terms emanating from the initial data and the nonhomogeneous term; and the remaining terms $w_{k+1}(x,y,t)$ for $k \geq 0$ follow recursively. Furthermore, the convergence of Adomian's method for the solution of functional equations has been proven long ago by a variety of researchers, including the references [38,39] to mention but a few.

3. Statement of the problem

In this section, we present three couplings based on the fractionalized two-dimensional heat diffusion models given in Eqs (1.3) and (1.4). The current couplings will pave the way to obtaining coupled systems of time-fractional two-dimensional heat diffusion models that will describe the diffusion process in a doubled-layered media.

3.1. Convective coupling model

Considering the individual fractionalized two-dimensional heat diffusion models in Eqs (1.3) and (1.4), the first coupling is made possible by introducing, and at the same time swapping the respective convective terms $\eta\frac{\partial w_1}{\partial y}$ and $\eta\frac{\partial w_2}{\partial y}$ in the models as follows

$$\begin{aligned}\frac{\partial^\alpha w_1}{\partial t^\alpha} &= \eta\frac{\partial w_2}{\partial y} + \frac{\partial^2 w_1}{\partial x^2} + \frac{\partial^2 w_1}{\partial y^2}, \quad 0 < \alpha \leq 1,\\ \frac{\partial^\alpha w_2}{\partial t^\alpha} &= \eta\frac{\partial w_1}{\partial y} + \frac{\partial^2 w_2}{\partial x^2} + \frac{\partial^2 w_2}{\partial y^2}, \quad 0 < \alpha \leq 1,\end{aligned} \tag{3.1}$$

couple with the following initial data

$$\begin{aligned}w_1 &= \sin(x)\sin(y), \quad \text{at} \quad t = 0,\\ w_2 &= \sin(x+y), \quad \text{at} \quad t = 0.\end{aligned} \tag{3.2}$$

Here, the convective coefficients η_1 and η_2 are presumed to be equal ($\eta_1 = \eta_2 = \eta$) for simplicity. Thus, η can equally be seen as an advection coefficient. Accordingly, we consider the convective coefficient η to be very small in order to examine the significance or otherwise of the coupling in relation to the original individual models; evidently, when $\eta \ll 1$, the respective exact solutions of the individual models are expected to be approached. Besides, the respective convective terms are expected to dominate the model when the convective coefficient η is very very large.

3.2. Nonlinear coupling model

Yet, we consider the individual fractionalized two-dimensional heat diffusion models as given in Eqs (1.3) and (1.4). However, in this case, the diffusivity constants in respective equations are assumed to be temperature-dependents. In fact, we swap the respective diffusivity constants and further express the models as follows

$$\begin{aligned}\frac{\partial^\alpha w_1}{\partial t^\alpha} &= \frac{\partial}{\partial x}\left(f(w_2)\frac{\partial w_1}{\partial x}\right) + \frac{\partial}{\partial y}\left(f(w_2)\frac{\partial w_1}{\partial y}\right), \quad 0 < \alpha \leq 1,\\ \frac{\partial^\alpha w_2}{\partial t^\alpha} &= \frac{\partial}{\partial x}\left(g(w_1)\frac{\partial w_2}{\partial x}\right) + \frac{\partial}{\partial y}\left(g(w_1)\frac{\partial w_2}{\partial y}\right), \quad 0 < \alpha \leq 1,\end{aligned} \tag{3.3}$$

couple with the following initial data

$$\begin{aligned}w_1 &= \sin(x)\sin(y), \quad \text{at} \quad t = 0,\\ w_2 &= \sin(x+y), \quad \text{at} \quad t = 0.\end{aligned} \tag{3.4}$$

In fact, the nonlinear terms $g(w_1)$ and $f(w_2)$ are both assumed to obey the power nonlinearity, that is [14]

$$g(w_1) = w_1^m, \qquad f(w_2) = w_2^n, \qquad m, n \in \mathbb{R}. \tag{3.5}$$

Indeed, the one-dimensional version of the corresponding integer-order model was studied by Bokhari et al. [14] using the classical Adomian decomposition. More so, the same power nonlinearity was used and mentioned that the power nonlinearities of $m = -1/2$ and $m = 2$ found applications in diffusion processes of plasma diffusion (and thermal expulsion of liquid Helium), and melting, together with the evaporation of metals, respectively.

3.3. Interfacial coupling model

Again, referring to the fractionalized heat diffusion models in Eqs (1.3) and (1.4), the present coupling is made possible by considering an infinite double-layered bar as shown in Figure 1. The double-layered bar is made of two different layers with the upper layer lying in $0 \leq y \leq h$, and the lower one occupying $-h \leq y \leq 0$.

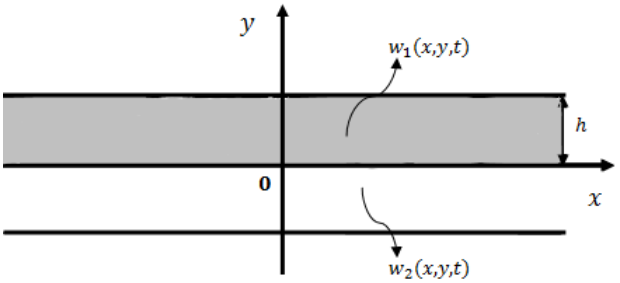

Figure 1. A double-layered bar.

Therefore, the related diffusional fields in the respective layers satisfy the following equations:

$$\begin{aligned} \frac{\partial^{\alpha} w_1}{\partial t^{\alpha}} &= \frac{\partial^2 w_1}{\partial x^2} + \frac{\partial^2 w_1}{\partial y^2}, \quad 0 < \alpha \leq 1, \\ \frac{\partial^{\alpha} w_2}{\partial t^{\alpha}} &= \frac{\partial^2 w_2}{\partial x^2} + \frac{\partial^2 w_2}{\partial y^2}, \quad 0 < \alpha \leq 1, \end{aligned} \tag{3.6}$$

and couple with the following initial data:

$$\begin{aligned} w_1 &= \sin(x)\sin(y), \quad \text{at} \quad t = 0, \\ w_2 &= \sin(x+y), \quad \text{at} \quad t = 0. \end{aligned} \tag{3.7}$$

Additionally, perfect continuity conditions between the two layers are further assumed at the interface ($y = 0$), which take the following prescription:

$$\begin{aligned} w_1 &= w_2 \quad \text{on} \quad y = 0, \\ \frac{\partial w_1}{\partial y} &= \frac{\partial w_2}{\partial y} \quad \text{on} \quad y = 0, \end{aligned} \tag{3.8}$$

where Eq $(3.8)_1$ means that the two diffusional fields are equal on the interface; while Eq $(3.8)_2$ states that the respective fluxes are equal on the same interface (remember that, both diffusivities κ_1 and κ_2 are initially assumed to be unity).

In addition, as the outer surface of the bar is assumed to be fully insulated, the respective fluxes in the two layers ($y = \pm h$) are bound to equal zero. In fact, the following insulation boundary conditions are imposed [27]:

$$\begin{aligned} \frac{\partial w_1}{\partial y} &= 0, \quad \text{on} \quad y = h, \\ \frac{\partial w_2}{\partial y} &= 0, \quad \text{on} \quad y = -h. \end{aligned} \tag{3.9}$$

4. Application

This section employs the outlined methodologies to treat the formulated fractionalized models for the two-dimensional heat diffusion processes earlier given in Eqs (1.3) and (1.4).

4.1. Laplace Adomian decomposition approach

In this subsection, we deploy the application of the Laplace Adomian decomposition approach to securitize the convective and nonlinear coupling models, respectively, of the related fractionalized heating model.

4.1.1. Convective coupling model

To solve the convective coupling model given in Eqs (3.1) and (3.2), we utilize the Laplace Adomian decomposition approach described earlier. Thus, without further delay, the following recursive solution is admitted by the governing model:

$$\begin{cases} w_{1_0}(x,y,t) = \sin(x)\sin(y), & k = 0, \\ w_{1_{k+1}}(x,y,t) = \mathfrak{L}^{-1}\left(s^{-\alpha}\left(\eta w^*_{2_{k_y}} + w^*_{1_{k_{xx}}} + w^*_{1_{k_{yy}}}\right)\right), & k \geq 0, \end{cases} \tag{4.1}$$

$$\begin{cases} w_{2_0}(x,y,t) = \sin(x+y), & k = 0, \\ w_{2_{k+1}}(x,y,t) = \mathfrak{L}^{-1}\left(s^{-\alpha}\left(\eta w^*_{1_{k_y}} + w^*_{2_{k_{xx}}} + w^*_{2_{k_{yy}}}\right)\right), & k \geq 0. \end{cases} \tag{4.2}$$

More so, certain explicit components are expressed from Eqs (4.1) and (4.2) as follow

$$
\begin{aligned}
w_{1_0}(x,y,t) &= \sin(x)\sin(y),\\
w_{1_1}(x,y,t) &= \mathfrak{Q}^{-1}\left(s^{-\alpha}\left(\eta w^*_{2_{0_y}} + w^*_{1_{0_{xx}}} + w^*_{1_{0_{yy}}}\right)\right)\\
&= \frac{t^{\alpha}(\eta\cos(x+y) - 2\sin(x)\sin(y))}{\Gamma(\alpha+1)},\\
w_{1_2}(x,y,t) &= \mathfrak{Q}^{-1}\left(s^{-\alpha}\left(\eta w^*_{2_{1_y}} + w^*_{1_{1_{xx}}} + w^*_{1_{1_{yy}}}\right)\right)\\
&= -\frac{t^{2\alpha}\left(\left(\eta^2-4\right)\sin(x)\sin(y) + 4\eta\cos(x+y)\right)}{\Gamma(2\alpha+1)},\\
w_{1_3}(x,y,t) &= \mathfrak{Q}^{-1}\left(s^{-\alpha}\left(\eta w^*_{2_{2_y}} + w^*_{1_{2_{xx}}} + w^*_{1_{2_{yy}}}\right)\right)\\
&= -\frac{t^{3\alpha}\left(2\left(4-3\eta^2\right)\sin(x)\sin(y) + \eta\left(\eta^2-12\right)\cos(x+y)\right)}{\Gamma(3\alpha+1)},\\
w_{1_4}(x,y,t) &= \mathfrak{Q}^{-1}\left(s^{-\alpha}\left(\eta w^*_{2_{3_y}} + w^*_{1_{3_{xx}}} + w^*_{1_{3_{yy}}}\right)\right)\\
&= \frac{t^{4\alpha}\left(8\eta\left(\eta^2-4\right)\cos(x+y) + \left(\eta^4-24\eta^2+16\right)\sin(x)\sin(y)\right)}{\Gamma(4\alpha+1)},\\
w_{1_5}(x,y,t) &= \mathfrak{Q}^{-1}\left(s^{-\alpha}\left(\eta w^*_{2_{4_y}} + w^*_{1_{4_{xx}}} + w^*_{1_{4_{yy}}}\right)\right)\\
&= \frac{t^{5\alpha}\left(\eta\left(\eta^4-40\eta^2+80\right)\cos(x+y) - 2\left(5\eta^4-40\eta^2+16\right)\sin(x)\sin(y)\right)}{\Gamma(5\alpha+1)},\\
w_{1_6}(x,y,t) &= \mathfrak{Q}^{-1}\left(s^{-\alpha}\left(\eta w^*_{2_{5_y}} + w^*_{1_{5_{xx}}} + w^*_{1_{5_{yy}}}\right)\right)\\
&= \frac{t^{6\alpha}\left(4\eta\left(3\eta^4-40\eta^2+48\right)\cos(x+y) + \left(\eta^6-60\eta^4+240\eta^2-64\right)\sin(x)\sin(y)\right)}{\Gamma(6\alpha+1)},\\
&\vdots
\end{aligned}
\tag{4.3}
$$

and

$$
\begin{aligned}
w_{2_0}(x,y,t) &= \sin(x+y),\\
w_{2_1}(x,y,t) &= \mathfrak{Q}^{-1}\left(s^{-\alpha}\left(\eta w^*_{1_{0_y}} + w^*_{2_{0_{xx}}} + w^*_{2_{0_{yy}}}\right)\right)\\
&= \frac{t^{\alpha}(\eta\sin(x)\cos(y) - 2\sin(x+y))}{\Gamma(\alpha+1)},\\
w_{2_2}(x,y,t) &= \mathfrak{Q}^{-1}\left(s^{-\alpha}\left(\eta w^*_{1_{1_y}} + w^*_{2_{1_{xx}}} + w^*_{2_{1_{yy}}}\right)\right)\\
&= -\frac{t^{2\alpha}\left(\left(\eta^2-4\right)\sin(x+y) + 4\eta\sin(x)\cos(y)\right)}{\Gamma(2\alpha+1)},\\
w_{2_3}(x,y,t) &= \mathfrak{Q}^{-1}\left(s^{-\alpha}\left(\eta w^*_{1_{2_y}} + w^*_{2_{2_{xx}}} + w^*_{2_{2_{yy}}}\right)\right)\\
&= -\frac{t^{3\alpha}\left(2\left(4-3\eta^2\right)\sin(x+y) + \eta\left(\eta^2-12\right)\sin(x)\cos(y)\right)}{\Gamma(3\alpha+1)},\\
w_{2_4}(x,y,t) &= \mathfrak{Q}^{-1}\left(s^{-\alpha}\left(\eta w^*_{1_{3_y}} + w^*_{2_{3_{xx}}} + w^*_{2_{3_{yy}}}\right)\right)\\
&= \frac{t^{4\alpha}\left(8\eta\left(\eta^2-4\right)\sin(x)\cos(y) + \left(\eta^4-24\eta^2+16\right)\sin(x+y)\right)}{\Gamma(4\alpha+1)},\\
w_{2_5}(x,y,t) &= \mathfrak{Q}^{-1}\left(s^{-\alpha}\left(\eta w^*_{1_{4_y}} + w^*_{2_{4_{xx}}} + w^*_{2_{4_{yy}}}\right)\right)\\
&= \frac{t^{5\alpha}\left(\eta\left(\eta^4-40\eta^2+80\right)\sin(x)\cos(y) - 2\left(5\eta^4-40\eta^2+16\right)\sin(x+y)\right)}{\Gamma(5\alpha+1)},\\
w_{2_6}(x,y,t) &= \mathfrak{Q}^{-1}\left(s^{-\alpha}\left(\eta w^*_{1_{5_y}} + w^*_{2_{5_{xx}}} + w^*_{2_{5_{yy}}}\right)\right)\\
&= \frac{t^{6\alpha}\left(4\eta\left(3\eta^4-40\eta^2+48\right)\sin(x)\cos(y) + \left(\eta^6-60\eta^4+240\eta^2-64\right)\sin(x+y)\right)}{\Gamma(6\alpha+1)},\\
&\vdots
\end{aligned}
\tag{4.4}
$$

Then, upon taking the net sums via the following expressions

$$
\begin{aligned}
w_1(x,y,t) &= \sum_{n=0}^{\infty} w_{1_n}(x,y,t),\\
w_2(x,y,t) &= \sum_{n=0}^{\infty} w_{2_n}(x,y,t),
\end{aligned}
\tag{4.5}
$$

the following resulting closed-form solution is yielded

$$
\begin{aligned}
w_1(x,y,t) &= \lambda_1(\alpha,t)\cos(x+y) + (E_\alpha(-2t) + \lambda_2(\alpha,t))\sin(x)\sin(y),\\
w_2(x,y,t) &= \lambda_1(\alpha,t)\sin(x)\sin(y) + (E_\alpha(-2t) + \lambda_2(\alpha,t))\sin(x+y),
\end{aligned}
\tag{4.6}
$$

where $E_\alpha(.)$ is the Mittag-Leffler function formally defined in Eq (1.5), and $\lambda_1(\alpha,t)$ and $\lambda_2(\alpha,t)$ are given by

$$
\lambda_1(\alpha,t) = \frac{\eta t^{\alpha}}{\Gamma(\alpha+1)} - \frac{4\eta t^{2\alpha}}{\Gamma(2\alpha+1)} - \frac{\eta\left(\eta^2-12\right)t^{3\alpha}}{\Gamma(3\alpha+1)} + \frac{8\eta\left(\eta^2-4\right)t^{4\alpha}}{\Gamma(4\alpha+1)} + \frac{\eta\left(\eta^4-40\eta^2+80\right)t^{5\alpha}}{\Gamma(5\alpha+1)} + \ldots \tag{4.7}
$$

$$\lambda_2(\alpha,t) = -\frac{\eta^2 t^{2\alpha}}{\Gamma(2\alpha+1)} + \frac{6\eta^2 t^{3\alpha}}{\Gamma(3\alpha+1)} - \frac{\left(24\eta^2-\eta^4\right)t^{4\alpha}}{\Gamma(4\alpha+1)} + \frac{\left(40\eta^2-5\eta^4\right)t^{5\alpha}}{\Gamma(5\alpha+1)} + \frac{\left(\eta^6-60\eta^4+240\eta^2\right)t^{6\alpha}}{\Gamma(6\alpha+1)} + \ldots \tag{4.8}$$

Moreover, as can be seen from Eqs (4.6)–(4.8), when $\eta = 0$, the expected convergent closed-form solution is recovered. Thus, to ensure a convergent solution, the convective coefficient η is thus constrained to be $\eta \ll 1$.

In what follows, we graphically portray the two-dimensional (2D) and three-dimensional (3D) visualizations for $w_1(x,y,t) = \sum_{n=0}^{15} w_{1_n}(x,y,t)$ and $w_2(x,y,t) = \sum_{n=0}^{15} w_{2_n}(x,y,t)$. In Figures 2 and 3, we give the 3D plots for (a) $w_1(x,y,t)$ and (b) $w_2(x,y,t)$ when $t = 0.5$ and $\alpha = 0.55$. Similarly, we give in Figures 4 and 5 the 2D plots for (a) $w_1(x,y,t)$ and (b) $w_2(x,y,t)$ when $t = 0.05$ and $y = 1$. Also, we set $\eta = 0.007$ and in Figures 2 and 4, and $\eta = 0.97$ and in Figures 3 and 5 to further study the effect of the convective coefficient parameter.

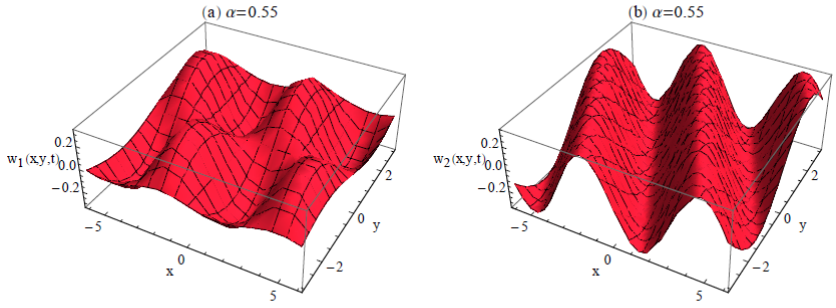

Figure 2. 3D visualization of the solution given in Eq (4.5) for (a) $w_1(x,y,t)$ and (b) $w_2(x,y,t)$ when $\eta = 0.007,\ \alpha = 0.55,\ t = 0.5$.

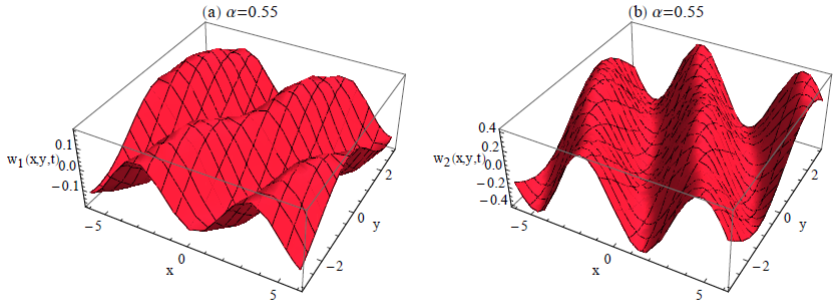

Figure 3. 3D visualization of the solution given in Eq (4.5) for (a) $w_1(x,y,t)$ and (b) $w_2(x,y,t)$ when $\eta = 0.97,\ \alpha = 0.55,\ t = 0.5$.

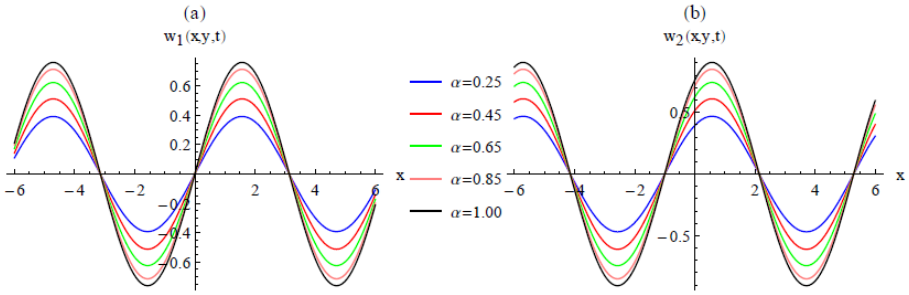

Figure 4. 2D visualization of the solution given in Eq (4.5) for (a) $w_1(x, y, t)$ and (b) $w_2(x, y, t)$ when $\eta = 0.007,\ y = 1,\ t = 0.05$.

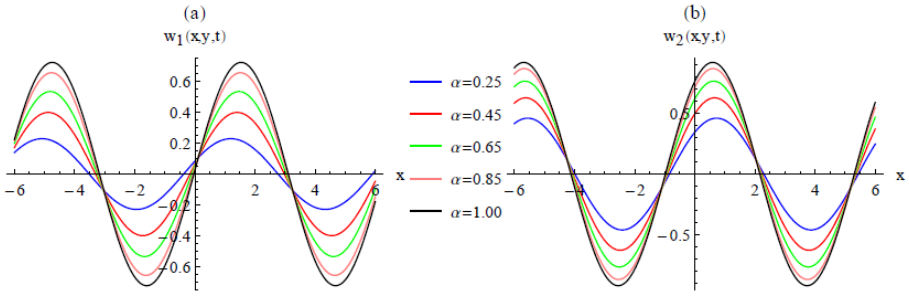

Figure 5. 2D visualization of the solution given in Eq (4.5) for (a) $w_1(x, y, t)$ and (b) $w_2(x, y, t)$ when $\eta = 0.97,\ y = 1,\ t = 0.05$.

4.1.2. Nonlinear coupling model

To solve the nonlinear coupling model given in Eqs (3.3)–(3.5), we make use of the same Laplace Adomian decomposition method. Indeed, the following recursive scheme is obtained

$$\begin{cases} w_{1_0}(x, y, t) = \sin(x)\sin(y), & k = 0, \\ w_{1_{k+1}}(x, y, t) = \mathfrak{L}^{-1}\left(s^{-\alpha}\mathfrak{L}\left(A_k + B_k + C_k\right)\right), & k \geq 0, \end{cases} \tag{4.9}$$

$$\begin{cases} w_{2_0}(x, y, t) = \sin(x + y), & k = 0, \\ w_{2_{k+1}}(x, y, t) = \mathfrak{L}^{-1}\left(s^{-\alpha}\mathfrak{L}\left(D_k + E_k + F_k\right)\right), & k \geq 0, \end{cases} \tag{4.10}$$

where A_k, B_k, C_k, D_k, E_k, and F_k are Adomian polynomials corresponding to the following respective nonlinear terms

$$\begin{aligned} A(w_1, w_2) &= w_2^n\left(\frac{\partial^2 w_1}{\partial x_2^2} + \frac{\partial^2 w_1}{\partial y_2^2}\right), & B(w_1, w_2) &= \frac{\partial}{\partial x}(w_2^n)\frac{\partial w_1}{\partial x}, & C(w_1, w_2) &= \frac{\partial}{\partial y}(w_2^n)\frac{\partial w_1}{\partial y}, \\ D(w_1, w_2) &= w_2^m\left(\frac{\partial^2 w_2}{\partial x_2^2} + \frac{\partial^2 w_2}{\partial y_2^2}\right), & E(w_1, w_2) &= \frac{\partial}{\partial x}(w_1^m)\frac{\partial w_2}{\partial x}, & F(w_1, w_2) &= \frac{\partial}{\partial y}(w_1^m)\frac{\partial w_2}{\partial y}. \end{aligned} \tag{4.11}$$

Moreover, these terms are to be computed using the generalized formula of the Adomian polynomials [10,28]. For instance, for A_k, we have the following expression

$$A_k = \frac{1}{k!}\frac{d^k}{d\zeta^k}\Big[N\Big(\sum_{j=0}^{\infty}\zeta^j w_j\Big)\Big]_{\zeta=0}, \quad k = 0, 1, 2, ... \tag{4.12}$$

Notetably, at $n = m = 0$, Eq (4.11) reduces to the following

$$A(w_1, w_2) = \frac{\partial^2 w_1}{\partial x_2^2} + \frac{\partial^2 w_1}{\partial y_2^2}, \qquad D(w_1, w_2) = \frac{\partial^2 w_2}{\partial x_2^2} + \frac{\partial^2 w_2}{\partial y_2^2}, \tag{4.13}$$

when

$$B(w_1, w_2) = C(w_1, w_2) = E(w_1, w_2) = F(w_1, w_2) = 0.$$

In such a situation, the governing nonlinear coupling model (now linear model) further admits the following recursive scheme as a special case

$$\begin{cases} w_{1_0}(x, y, t) = \sin(x)\sin(y), & k = 0, \\ w_{1_{k+1}}(x, y, t) = \mathfrak{L}^{-1}\left(s^{-\alpha}\left(w^*_{1_{k_{xx}}} + w^*_{1_{k_{yy}}}\right)\right), & k \geq 0, \end{cases} \tag{4.14}$$

$$\begin{cases} w_{2_0}(x, y, t) = \sin(x + y), & k = 0, \\ w_{2_{k+1}}(x, y, t) = \mathfrak{L}^{-1}\left(s^{-\alpha}\mathfrak{L}\left(w^*_{2_{k_{xx}}} + w^*_{2_{k_{yy}}}\right)\right), & k \geq 0, \end{cases} \tag{4.15}$$

which are the obvious solutions of the uncoupled models. More so, as the present solution goes hand-in-hand with that of the previous subsection, with regard to the methodology, we, therefore, deem not to dissect it in this scenario. Additionally, Bokhari et al. [14] have provided a sufficient explanation about the one-dimensional version of the corresponding integer-order model, including the coding for the numerical simulation and analysis.

4.2. Integral transforms method on interfacial coupling model

Now, taking the Laplace and Fourier transforms in t- and x-variables simultaneously in Eq (3.6), the model reduces to the system of second-order differential equations as follows

$$\begin{aligned} \frac{\partial^2 \bar{w}^*_1}{\partial y^2} - r^2\bar{w}^*_1 &= -i\sqrt{\frac{\pi}{2}}\delta(q-1)s^{\alpha-1}\sin(y), \\ \frac{\partial^2 \bar{w}^*_2}{\partial y^2} - r^2\bar{w}^*_2 &= -i\sqrt{\frac{\pi}{2}}\delta(q-1)s^{\alpha-1}e^{-iqy}, \end{aligned} \tag{4.16}$$

where $i = \sqrt{-1}$, $r = \sqrt{q^2 + s^\alpha}$ and $\delta(q-1)$ is a Dirac delta function for $q > 1$, which appears as a result of taking the Fourier transform in x; remember also that the Dirac delta function satisfies

$$\int_{-\infty}^{\infty} f(q)\delta(q - q_0)dq = f(q_0). \tag{4.17}$$

Similarly, the Laplace-Fourier transformed interfacial and boundary data take the following expression

$$\bar{w}_1 = \bar{w}^*_2 \quad \text{and} \quad \frac{\partial \bar{w}^*_1}{\partial y} = \frac{\partial \bar{w}_2}{\partial y} \quad \text{on} \quad y = 0, \tag{4.18}$$

and

$$\frac{\partial \bar{w}_1^*}{\partial y} = 0 \quad \text{on} \quad y = h, \quad \text{and} \quad \frac{\partial \bar{w}_2^*}{\partial y} = 0 \quad \text{on} \quad y = -h. \tag{4.19}$$

Therefore, the system of second-order differential equations given in Eq (4.16) admits the following exact transformed solutions

$$\begin{aligned} \bar{w}_1^*(q, y, s) &= A_1 e^{ry} + A_2 e^{-ry} + i\sqrt{\frac{\pi}{2}} \frac{s^{\alpha-1}\delta(q-1)}{r^2+1} \sin(y), \\ \bar{w}_2^*(q, y, s) &= B_1 e^{ry} + B_2 e^{-ry} + i\sqrt{\frac{\pi}{2}} \frac{s^{\alpha-1}\delta(q-1)}{s^\alpha + 2q^2} e^{-iqy}, \end{aligned} \tag{4.20}$$

where A_d, and B_d for $d = 1, 2$ are constants to be found from the prescribed conditions.

Additionally, if we apply the transformed continuity and insulation boundary conditions given in Eqs (4.18) and (4.19) to Eq (4.20), the following system of algebraic linear equations is posed

$$A\mathbf{x} = b, \tag{4.21}$$

where

$$A = \begin{pmatrix} 1 & 1 & -1 & -1 \\ 1 & -1 & -1 & 1 \\ e^{hr} & -e^{-hr} & 0 & 0 \\ 0 & 0 & e^{-hr} & -e^{hr} \end{pmatrix}, \qquad \mathbf{x} = \begin{pmatrix} A_1 \\ A_2 \\ B_1 \\ B_2 \end{pmatrix}, \tag{4.22}$$

and

$$b = \sqrt{\frac{\pi}{2}} s^{\alpha-1}\delta(q-1) \begin{pmatrix} \frac{i}{s^\alpha+2q^2} \\ -\frac{1}{r}\left(\frac{i}{r^2+1} - \frac{1}{s^\alpha+2}\right) \\ -\frac{i\cos(h)}{r\left(r^2+1\right)} \\ -\frac{e^{ih}}{r(s^\alpha+2)} \end{pmatrix}. \tag{4.23}$$

Moreover, Eq (4.21) admits the following solution

$$\mathbf{x} = A^{-1}b, \tag{4.24}$$

where

$$A^{-1} = (2e^{2hr}(1 - e^{-4hr}))^{-1} \begin{pmatrix} 1 - e^{-2hr} & -1 - e^{-2hr} & 2e^{hr} & -2e^{-hr} \\ -1 + e^{2hr} & -1 - e^{2hr} & 2e^{-hr} & -2e^{hr} \\ 1 - e^{2hr} & -1 - e^{2hr} & 2e^{hr} & -2e^{-hr} \\ -1 + e^{-2hr} & -1 - e^{-2hr} & 2e^{-hr} & -2e^{hr} \end{pmatrix}. \tag{4.25}$$

For explicit expression of $\mathbf{x} = (A_1, A_2, B_1, B_2)^T$, see Appendix A.

Therefore, having determined the expressions for A_1, A_2, B_1, and B_2, we thus return to Eq (4.20) to reverse the solution back to the original domain, that is, $(p, y, s) \to (x, y, t)$. In doing so, we start off by applying the inverse Fourier transform to Eq (4.20) to reveal

$$\begin{aligned} w_1^*(x, y, s) &= \frac{s^{\alpha-1}}{8\left(s^\alpha + 2\right)} e^{-ix}\left(\gamma_1 e^{-y\sqrt{s^\alpha+1}} + \gamma_2 e^{y\sqrt{s^\alpha+1}} + 4i\sin(y)\right), \\ w_2^*(x, y, s) &= \frac{s^{\alpha-1}}{8\left(s^\alpha + 2\right)} e^{-ix}\left(\gamma_3 e^{-y\sqrt{s^\alpha+1}} + \gamma_4 e^{(h+y)\sqrt{s^\alpha+1}} + 4ie^{-iy}\right), \end{aligned} \tag{4.26}$$

where $\gamma,\gamma_2, \gamma_3$ and γ_4 are given Appendix B.

Next, employing the inverse Laplace transform on Eq (4.26), one gets

$$\begin{aligned} w_1(x,y,t) &= \frac{e^{-ix}}{16\pi i}\int_{c-i\infty}^{c+i\infty}\left(\frac{s^{\alpha-1}}{s^\alpha+2}\left(\gamma_1 e^{-y\sqrt{s^\alpha+1}}+\gamma_2 e^{y\sqrt{s^\alpha+1}}+4i\sin(y)\right)\right)ds, \quad c>0,\\ w_2(x,y,t) &= \frac{e^{-ix}}{16\pi i}\int_{c-i\infty}^{c+i\infty}\left(\frac{s^{\alpha-1}}{s^\alpha+2}\left(\gamma_3 e^{-y\sqrt{s^\alpha+1}}+\gamma_4 e^{(h+y)\sqrt{s^\alpha+1}}+4ie^{-iy}\right)\right)ds, \quad c>0. \end{aligned} \tag{4.27}$$

We mention here that the Laplace inversion of Eq (4.27) is not possible analytically! However, we seek a numerical inversion algorithm to carry out this task. Thus, we get hold of one of the powerful numerical algorithms by Abate and Valkó [31]. In [31], an efficient algorithm was proposed that numerically inverts Laplace transform at a given point, say at t_p. More, the *Mathematica* software is deplored for the simulation.

More so, we graphically portray the 2D and 3D visualizations of the solutions $w_1(x,y,t)$ and $w_2(x,y,t)$ determined in Eq (4.27) at $t = 0.5$. In Figures 6 and 7, we give the 3D surfaces for (a) $w_1(x,y,t)$ and (b) $w_2(x,y,t)$ at $\alpha = 0.45$ and $\alpha = 0.85$, correspondingly. Similarly, we depict in Figure 8 the 2D plots for (a) $w_1(x,y,t)$ and (b) $w_2(x,y,t)$ when $y = 1$ for various values of α.

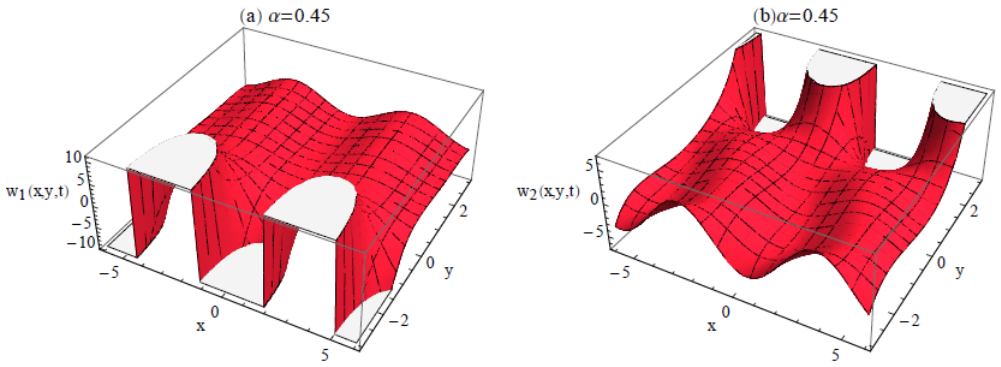

Figure 6. 3D visualization of the solution given in Eq (4.27) for (a) $w_1(x,y,t)$ and (b) $w_2(x,y,t)$ when $\alpha = 0.45$.

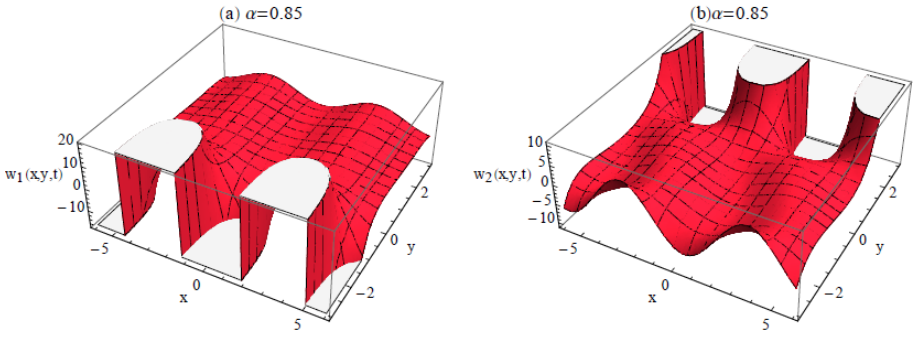

Figure 7. 3D visualization of the solution given in Eq (4.27) for (a) $w_1(x, y, t)$ and (b) $w_2(x, y, t)$ when when $\alpha = 0.85$.

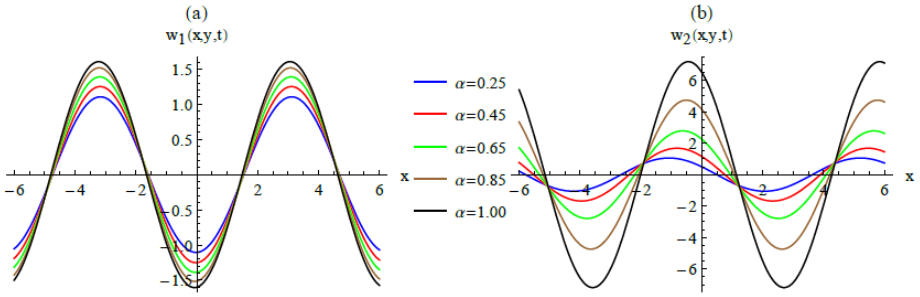

Figure 8. 2D visualization of the solution given in Eq (4.27) for (a) $w_1(x, y, t)$ and (b) $w_2(x, y, t)$ at $y = 1$ for various values of when α.

5. Conclusions

In conclusion, the present manuscript gave a complete overview of the two-dimensional heat diffusion models that underwent a fractional transformation, system coupling, as well as solution treatment. Two heat diffusion models were considered and endowed with Caputo's fractional-order derivatives in time t, and further coupled using the ideas of the convection-diffusion process, nonlinear coupling, and also the idea of interfacial coupling-making consideration to the dynamics of an infinite double-layered thermoelastic bar. The Laplace Adomian decomposition approach and the integral transformation method were employed to study the respective models. Further, these methods have various advantages in their own rights, including rapid convergence to the exact solution, and the fact that they neither need discretization nor linearization to reach the expected closed-form solution, to state a few. Thus, graphical illustrations were presented to graphically view the obtained solutions, and thereafter, described the significance of the fractional orders on the respective fields. All-in-all, we draw the following observations:

1) The first coupled model with regard to the convection-diffusion idea behaved more like the respective individual models when $\eta << 1$, and far away when $\eta >> 1$; see Figures 2–5. In fact, this is so because when $\eta = 0$, both $\lambda_1(\alpha, t)$ and $\lambda_2(\alpha, t)$ varnish from Eq (4.6); which evidently, the diffusional fields $w_1(x, y, t)$ and $w_2(x, y, t)$ return the exact solutions of the original models.
2) The second coupling entailed nonlinear coupling due to temperature-dependent diffusivities. The Laplace Adomian decomposition method was used to recurrently determine the resulting solution in compact form. Such situations have been reported to be applicable to various media, like gases, where the thermal parameters are found to be proportional to the temperature of the media [14].
3) The third coupled model for the double-layered bar also worked fine analytically; only the analytical Laplace inversion was not possible. However, everything went smoothly upon employing the computational Laplace inversion algorithm [31]. The significance of the fractional-order derivative on the diffusional fields $w_1(x, y, t)$ and $w_2(x, y, t)$ (determined in Eq (4.26) were shown in Figures 6–8. In Figures 6 and 7, certain singular regions were noted that might arise from the Laplace inversion.

Conclusively, the present study can be applied to various thermodynamical models in thermoelasticity, especially in the design/fabrication and modeling of multilayered thermoelastic structures. Moreover, the present study also fits the application of heat diffusion scenarios, including modeling anomalies and cancer tumors in heterogeneous media.

Acknowledgements

J. F. Gómez-Aguilar acknowledges the support provided by CONACyT: cátedras CONACyT para jóvenes investigadores 2014 and SNI-CONACyT.

Conflict of interest

The authors declare no conflict of interest.

Code availability

Not applicable.

Authors' Contributions

R.I. Nuruddeen, J.F. Gómez-Aguilar, José R. Razo-Hernández: Conceptualization, Methodology, Writing- Original draft preparation, Methodology, Data curation, Supervision. All authors read and approved the final manuscript.

Ethics approval

Not applicable.

Consent to participate

All authors approved the final manuscript.

Consent for publication

All authors approved the publication of the manuscript.

Appendix A

The following are the determined expressions for the unknowns A_1, A_2, B_1 and B_2 in Eq (4.20) that are obtained from Eq (4.24):

$$A_1 = \frac{\sqrt{\frac{\pi}{2}}\delta(q-1)s^{\alpha-1}e^{h\left(\sqrt{s^\alpha+1}+i\right)}}{\sqrt{s^\alpha+1}\,(s^\alpha+2)\left(e^{4h\sqrt{s^\alpha+1}}-1\right)} - \frac{i\sqrt{\frac{\pi}{2}}\delta(q-1)\cos(h)s^{\alpha-1}e^{3h\sqrt{s^\alpha+1}}}{\sqrt{s^\alpha+1}\,(s^\alpha+2)\left(e^{4h\sqrt{s^\alpha+1}}-1\right)} - \frac{i\sqrt{\frac{\pi}{2}}\delta(q-1)s^{\alpha-1}\left(\tanh\left(h\sqrt{s^\alpha+1}\right)-1\right)}{4\,(s^\alpha+2)} - \frac{\left(\frac{1}{4}-\frac{i}{4}\right)\sqrt{\frac{\pi}{2}}\delta(q-1)s^{\alpha-1}\left(\coth\left(h\sqrt{s^\alpha+1}\right)-1\right)}{\sqrt{s^\alpha+1}\,(s^\alpha+2)},$$

$$A_2 = \frac{\sqrt{\frac{\pi}{2}}i\delta(q-1)s^{\alpha-1}e^{2h\sqrt{s^\alpha+1}}}{2\,(s^\alpha+2)\left(e^{2h\sqrt{s^\alpha+1}}+1\right)} + \frac{\sqrt{\frac{\pi}{2}}\delta(q-1)s^{\alpha-1}e^{h\left(3\sqrt{s^\alpha+1}+i\right)}}{\sqrt{s^\alpha+1}\,(s^\alpha+2)\left(e^{4h\sqrt{s^\alpha+1}}-1\right)} - \frac{i\sqrt{\frac{\pi}{2}}\delta(q-1)\cos(h)s^{\alpha-1}e^{h\sqrt{s^\alpha+1}}}{\sqrt{s^\alpha+1}\,(s^\alpha+2)\left(e^{4h\sqrt{s^\alpha+1}}-1\right)} - \frac{\left(\frac{1}{4}-\frac{i}{4}\right)\sqrt{\frac{\pi}{2}}\delta(q-1)s^{\alpha-1}e^{2h\sqrt{s^\alpha+1}}\left(\coth\left(h\sqrt{s^\alpha+1}\right)-1\right)}{\sqrt{s^\alpha+1}\,(s^\alpha+2)},$$

$$B_1 = \frac{\sqrt{\frac{\pi}{2}}\delta(q-1)s^{\alpha-1}e^{h\left(\sqrt{s^\alpha+1}+i\right)}}{\sqrt{s^\alpha+1}\,(s^\alpha+2)\left(e^{4h\sqrt{s^\alpha+1}}-1\right)} - \frac{i\sqrt{\frac{\pi}{2}}\delta(q-1)s^{\alpha-1}e^{2h\sqrt{s^\alpha+1}}}{2\,(s^\alpha+2)\left(e^{2h\sqrt{s^\alpha+1}}+1\right)} - \frac{i\sqrt{\frac{\pi}{2}}\delta(q-1)\cos(h)s^{\alpha-1}e^{3h\sqrt{s^\alpha+1}}}{\sqrt{s^\alpha+1}\,(s^\alpha+2)\left(e^{4h\sqrt{s^\alpha+1}}-1\right)} - \frac{\left(\frac{1}{4}-\frac{i}{4}\right)\sqrt{\frac{\pi}{2}}\delta(q-1)s^{\alpha-1}e^{2h\sqrt{s^\alpha+1}}\left(\coth\left(h\sqrt{s^\alpha+1}\right)-1\right)}{\sqrt{s^\alpha+1}\,(s^\alpha+2)},$$

$$B_2 = \frac{\sqrt{\frac{\pi}{2}}\delta(q-1)s^{\alpha-1}e^{h\left(3\sqrt{s^\alpha+1}+i\right)}}{\sqrt{s^\alpha+1}\,(s^\alpha+2)\left(e^{4h\sqrt{s^\alpha+1}}-1\right)} - \frac{i\sqrt{\frac{\pi}{2}}\delta(q-1)\cos(h)s^{\alpha-1}e^{h\sqrt{s^\alpha+1}}}{\sqrt{s^\alpha+1}\,(s^\alpha+2)\left(e^{4h\sqrt{s^\alpha+1}}-1\right)} + \frac{i\sqrt{\frac{\pi}{2}}\delta(q-1)s^{\alpha-1}\left(\tanh\left(h\sqrt{s^\alpha+1}\right)-1\right)}{4\,(s^\alpha+2)} - \frac{\left(\frac{1}{4}-\frac{i}{4}\right)\sqrt{\frac{\pi}{2}}\delta(q-1)s^{\alpha-1}\left(\coth\left(h\sqrt{s^\alpha+1}\right)-1\right)}{\sqrt{s^\alpha+1}\,(s^\alpha+2)}.$$

Appendix B

The expressions for $\gamma_1, \gamma_2, \gamma_3$ and γ_4 in Eqs (4.26) and (4.27) are given by:

$$\gamma_1 = \frac{-2ie^{h\left(\sqrt{s^\alpha+1}-i\right)} - 2ie^{h\left(\sqrt{s^\alpha+1}+i\right)} + 4e^{h\left(3\sqrt{s^\alpha+1}+i\right)}}{\sqrt{s^\alpha+1}\left(e^{4h\sqrt{s^\alpha+1}}-1\right)} + \frac{2i\left(\sqrt{s^\alpha+1}+(1+i)\right)e^{4h\sqrt{s^\alpha+1}} - 2i\left(\sqrt{s^\alpha+1}+(-1-i)\right)e^{2h\sqrt{s^\alpha+1}}}{\sqrt{s^\alpha+1}\left(e^{4h\sqrt{s^\alpha+1}}-1\right)},$$

$$\gamma_2 = \frac{4e^{h\left(\sqrt{s^\alpha+1}+i\right)} - 2i\sqrt{s^\alpha+1} + (-2+2i)}{\sqrt{s^\alpha+1}\left(e^{4h\sqrt{s^\alpha+1}}-1\right)} + \frac{2i\left(\sqrt{s^\alpha+1}+(1+i)\right)e^{2h\sqrt{s^\alpha+1}} - 4i\cos(h)e^{3h\sqrt{s^\alpha+1}}}{\sqrt{s^\alpha+1}\left(e^{4h\sqrt{s^\alpha+1}}-1\right)},$$

$$\gamma_3 = \frac{-2ie^{h\left(\sqrt{s^\alpha+1}-i\right)} - 2ie^{h\left(\sqrt{s^\alpha+1}+i\right)} + 4e^{h\left(3\sqrt{s^\alpha+1}+i\right)}}{\sqrt{s^\alpha+1}\left(e^{4h\sqrt{s^\alpha+1}}-1\right)} + \frac{2i\left(\sqrt{s^\alpha+1}+(1+i)\right) - 2i\left(\sqrt{s^\alpha+1}+(-1-i)\right)e^{2h\sqrt{s^\alpha+1}}}{\sqrt{s^\alpha+1}\left(e^{4h\sqrt{s^\alpha+1}}-1\right)},$$

$$\gamma_4 = \frac{4e^{ih} - 2i\left(\sqrt{s^\alpha+1}+(-1-i)\right)e^{3h\sqrt{s^\alpha+1}}}{\sqrt{s^\alpha+1}\left(e^{4h\sqrt{s^\alpha+1}}-1\right)} + \frac{2i\left(\sqrt{s^\alpha+1}+(1+i)\right)e^{h\sqrt{s^\alpha+1}} - 4i\cos(h)e^{2h\sqrt{s^\alpha+1}}}{\sqrt{s^\alpha+1}\left(e^{4h\sqrt{s^\alpha+1}}-1\right)}.$$

References

1. D. R. Poirier,G. H. Geiger, Conduction of heat in solids, In: *Transport Phenomena in Materials Processing*, Springer, 2016, 281–327. https://doi.org/10.1007/978-3-319-48090-9_9
2. R. I. Nuruddeen, Approximate analytical solution to the Cattaneo heat conduction model with various laser sources, *J. Appl. Math. Comput. Mech.*, **22** (2022), 67–78. http://doi.org/10.17512/jamcm.2022.1.06
3. R. I. Nuruddeen, F. D. Zaman, Temperature distribution in a circular cylinder with general mixed boundary conditions, *J. Multidiscip. Eng. Sci. Technol.*, **3** (2016), 3653–3658.
4. H. R. Al-Duhaim, F. D. Zaman, R. I. Nuruddeen, Thermal stress in a half-space with mixed boundary conditions due to time dependent heat source, *J. Math.*, **11** (2015), 19–25. http://doi.org/10.9790/5728-11651925

5. L. Debnath, Recent applications of fractional calculus to science and engineering, *Int. J. Math. Math. Sci.*, **2003** (2003), 3413–3442. https://doi.org/10.1155/S0161171203301486

6. A. A. Kilbas, H. M. Srivastava, J. J. Trujillo, *Theory and Applications of Fractional Differential Equations*, Elsevier, 2006.

7. R. Khalil, M. Al Horani, A. Yousef, M. Sababheh, A new definition of fractional derivative, *J. Comput. Appl. Math.*, **264** (2014), 65–701. https://doi.org/10.1016/j.cam.2014.01.002

8. A. Atangana, D. Baleanu, New fractional derivatives with nonlocal and non-singular kernel: Theory and application to heat transfer model, *Therm. Sci.*, **20** (2016), 763–769. https://doi.org/10.2298/TSCI160111018A

9. K. R. Raslan, K. A. Khalid, M. A. Shallal, The modified extended tanh method with the Riccati equation for solving the space-time fractional EW and MEW equations, *Chaos Solitons Fractals*, **103** (2017), 404–409. https://doi.org/10.1016/j.chaos.2017.06.029

10. R. I. Nuruddeen, Y. Akbar, H. J. Kim, On the application of G_α integral transform to nonlinear dynamical models with non-integer order derivatives, *AIMS Mathematics* , **7** (2022), 17859–17878. https://doi.org/10.3934/math.2022984

11. S. P. Yan, W. P. Zhong, X. J. Yang, A novel series method for fractional diffusion equation within Caputo fractional derivative, *Therm. Sci.*, **20** (2016), S695–S699. https://doi.org/10.2298/TSCI16S3695Y

12. K. Al-Khaled, S. Momani, An approximate solution for a fractional diffusion-wave equation using the decomposition method, *Appl. Math. Comput.*, **165** (2005), 473–483. https://doi.org/10.1016/j.amc.2004.06.026

13. S. S. Ray, R. K. Bera, Analytical solution of a fractional diffusion equation by Adomian decomposition method, *Appl. Math. Comput.*, **174** (2006), 329–336. https://doi.org/10.1016/j.amc.2005.04.082

14. A. H. Bokhari, G. Mohammad, M. T. Mustafa, F. D. Zaman, Adomian decomposition method for a nonlinear heat equation with temperature dependent thermal properties, *Math. Probl. Eng.*, **2009** (2009), 926086. https://doi.org/10.1155/2009/926086

15. A. H. Bokhari, G. Mohammad, M. T. Mustafa, F. D. Zaman, Solution of heat equation with nonlocal boundary conditions, *Int. J. Math. Comput.*, **3** (2009), 100–113.

16. R. I. Nuruddeen, F. D. Zaman, Y. F. Zakariya, Analysing the fractional heat diffusion equation solution in comparison with the new fractional derivative by decomposition method, *Malaya J. Matematik*, **7** (2019), 213–222. https://doi.org/10.26637/MJM0702/0012

17. A. M. Wazwaz, Exact solutions to nonlinear diffusion equations obtained by the decomposition method, *Appl. Math. Comput.*, **123** (2001), 109–122. https://doi.org/10.1016/S0096-3003(00)00064-3

18. R. I. Nuruddeen, B. D. Garba, Analytical technique for (2+1) fractional diffusion equation with nonlocal boundary conditions, *Open J. Math. Sci.*, **2** (2018), 287–300. http://doi.org/10.30538/oms2018.0035

19. A. Ahmad, A. H. Bokhari, A. H. Kara, F. D. Zaman, Symmetry classifications and reductions of some classes of (2+1)-nonlinear heat equation, *J. Math. Anal. Appl.*, **339** (2008), 175–181. https://doi.org/10.1016/j.jmaa.2007.07.002
20. M. Caputo, Diffusion of fluids in porous media with memory, *Geothermics*, **28** (1999), 113–130. https://doi.org/10.1016/S0375-6505(98)00047-9
21. P. S. Laplace, *Theorie Analytique des Probabilities*, 1820.
22. D. Bhatta, *Integral Transforms and their Applications*, New York: Springer New York, 2002. https://doi.org/10.1007/978-1-4684-9283-5
23. H. Eltayeb, K. Adem, M. Said, Modified Laplace decomposition method for solving systems of equations Emden-Fowler type, *J. Comput. Theor. Nanos.*, **12** (2015), 5297–5301. http://doi.org/10.1166/jctn.2015.4518
24. S. A. Khuri, A Laplace decomposition algorithm applied to a class of nonlinear defferential equations, *J. Appl. Math.*, **4** (2001), 141–155. https://doi.org/10.1155/S1110757X01000183
25. S. Islam, Y. Khan, N. Faraz, F. Austin, Numerical solution of logistic differential equations by using the Laplace decomposition method, *World Appl. Sci. J.*, **8** (2010), 1100–1105.
26. R. I. Nuruddeen, L. Muhammad, A. M. Nass, T. A. Sulaiman, A review of the integral transforms-based decomposition methods and their applications in solving nonlinear PDEs, *Palestine J. Math.*, **7** (2018), 262–280.
27. K. Masood, F. D. Zaman, Initial inverse problem in a two-layer heat conduction model, *Arab. J. Sci. Eng.*, **29** (2004), 3–12.
28. G. Adomian, A review of the decomposition method in applied mathematics, *J. Math. Anal. Appl.*, **135** (1988), 501–544. https://doi.org/10.1016/0022-247X(88)90170-9
29. A. Al Qarni, M. A. Banaja, H. O. Bakodah, A. A. Alshaery, Q. Zhou, A. Biswas, et al., Bright optical solitons for Lakshmanan-Porsezian-Daniel model with spatio-temporal dispersion by improved Adomian decomposition method, *Optik*, **181** (2019), 891–897. https://doi.org/10.1016/j.ijleo.2018.12.172
30. H. O. Bakodah, M. A. Banaja, A. A. Alshaery, A. A. Al Qarni, Numerical solution of dispersive optical solitons with Schrödinger-Hirota equation by improved Adomian decomposition method, *Math. Probl. Eng.*, **2019** (2019), 2960912. https://doi.org/10.1155/2019/2960912
31. J. Abate, P. P. Valkó, Multi-precision Laplace transform inversion, *Internat. J. Numer. Methods Engrg.*, **60** (2004), 979–993. https://doi.org/10.1002/nme.995
32. R. I. Nuruddeen, Laplace-based method for the linearized dynamical models in the presence of Hilfer fractional operator, *Partial Differ. Eq. Appl. Math.*, **5** (2022), 100248. https://doi.org/10.1016/j.padiff.2021.100248
33. N. Ahmed, N. A. Shah, S. Teherifar, F. D. Zaman, Memory effects and of the killing rate on the tumor cells concentration for a one-dimensional cancer model, *Chaos Solitons Fractal*, **144** (2021), 110750. https://doi.org/10.1016/j.chaos.2021.110750
34. A. S. M. Alzaidi, A. M. Mubaraki, R. I. Nuruddeen, Effect of fractional temporal variation on the vibration of waves on elastic substrates with spatial non-homogeneity, *AIMS Mathematics*, **7** (2022), 13746–13762. https://doi.org/10.3934/math.2022757

35. S. Althobaiti, A. Mubaraki, R. I. Nuruddeen, J. F. Gómez-Aguilar, Wave propagation in an elastic coaxial hollow cylinder when exposed to thermal heating and external load, *Results Phys.*, **38** (2022), 105582. https://doi.org/10.1016/j.rinp.2022.105582

36. H. Stehfest, Remarks on algorithm 368: Numerical inversion of Laplace transform, *Commun. ACM*, **13** (1970). https://doi.org/10.1145/355598.362787

37. V. Masol, J. L. Teugels, Numerical accuracy of real inversion formulas for the Laplace transform, *J. Comput. Appl. Math.*, **233** (2010), 2521–2533. https://doi.org/10.1016/j.cam.2009.10.033

38. Y. Cherruault, Convergence of Adomian's method, *Math. Comput. Model.*, **14** (1990), 83–86. https://doi.org/10.1016/0895-7177(90)90152-D

39. K. Abbaoui, Y. Cherruault, Convergence of Adomian's method applied to nonlinear equations, *Math. Comput. Model.*, **20** (1994), 69–73. https://doi.org/10.1016/0895-7177(94)00163-4

AIMS Press

© 2023 the Author(s), licensee AIMS Press. This is an open access article distributed under the terms of the Creative Commons Attribution License (http://creativecommons.org/licenses/by/4.0)